

# Selective Storage of Magnetization in Strongly Relaxing Spin Systems

M. L. Kilfoil\* and P. T. Callaghan†

\*Physics and Physical Oceanography, Memorial University of Newfoundland, St. John's, Newfoundland A1B 3X7, Canada; and †Institute of Fundamental Sciences–Physics, Massey University, Palmerston North, New Zealand

Received July 14, 2000; revised January 23, 2001; published online May 10, 2001

**We have investigated the use of a “split-sinc” RF pulse to selectively store magnetization from a selected region of a sample, for later recall in imaging or spectroscopy experiments. The pulse sequence is based on an original suggestion by Post *et al.* (West German Patent No. P3209263.6, 13 March 1982), later implemented by Aue *et al.* (*J. Magn. Reson.* **56**, 350 (1984)). We have carried out detailed numerical calculations using the Bloch equations and show that this particular sequence is robust in the face of strong transverse relaxation, and we demonstrate its application to imaging of polymer samples in shearing and extensional flow cells.** © 2001 Academic Press

## INTRODUCTION

Localized NMR spectroscopy depends on the use of a frequency-selective radiofrequency (RF) pulse applied in the presence of a magnetic field gradient, so that only spins from a desired region of the sample participate in the NMR spectrum. Such localized spectroscopy is extensively used in biomedical magnetic resonance, where a wide variety of excitation methods are successfully employed (1–5). All of these methods involve a pulse sequence whose frequency selectivity arises from a finite pulse bandwidth which bears an inverse relationship to the pulse duration. Because of the need for finite duration pulses, the issue of spin relaxation during the excitation process can be important. Most sequences cause the spin magnetization of interest (in the desired region) to execute a complex trajectory in Cartesian space in which the respective durations of transverse and longitudinal components determine the degree of  $T_2$  and  $T_1$  relaxation.

In this article we consider the special case where the spins of interest suffer strong  $T_2$  relaxation but relatively weak  $T_1$  relaxation, so that we seek to minimize the time that components of the desired magnetization reside in the transverse plane. The particular focus of application is in the “Rheo-NMR” (6, 7) studies of soft condensed matter such as polymers and liquid crystals, systems for which the intermediate motional narrowing leads to  $T_2 \ll T_1$ . The use of magnetic resonance spectroscopy in rheological investigations is relatively new. Its strength lies in an ability to report on molecular, as opposed to bulk, information about induced and often weak alignment of complex fluids under flow.

The need to select different regions of fluid is crucial in studies of molecular ordering in which order is measured along different directions of the principal axis system of the molecule. Both the proton dipolar interaction and the deuterium quadrupolar interaction can provide information regarding local alignment, and since these are first-order perturbations to the spin Hamiltonian, these are always projected along the polarizing field axis associated with the zeroth-order Zeeman interaction. Two examples of relevant geometries are shown in Fig. 1. In one case we seek to measure the local alignment in a Couette cell, selecting a region where the velocity and velocity gradient axes have a defined angle with respect to  $B_0$ . This requires that we select a strip of spins corresponding to the desired orientation. In the other case we wish to measure the local alignment for spins near the stagnation point in a four-roll mill, in which the extensional strain field is highly nonuniform. We wish to select a defined area of sample near the cell center where the flow field is very nearly homogeneous. Both cases will be addressed in the experimental section of this paper.

## SELECTIVE STORAGE SEQUENCE

Spatial selection methods typically employ low-power frequency-selective pulses to excite a well-defined slice or volume element. Such pulses expose the desired spins to the negative effects of dephasing and transverse relaxation for a proportion of the pulse duration, and this may lead to significant signal loss. In situations that require several selective pulses to be applied in sequence, e.g., for selection in two or three orthogonal directions, these problems compound. Ideally, the selection part of the pulse sequence must be fast enough to avoid excessive decays of the observable signal. In cases where  $T_2$  is on the order of milliseconds to tens of milliseconds, the decay can be severe.

Our spatial localization method is based on a composite soft/hard pulse “selective storage” proposed by Post *et al.* (8) and first implemented by Aue *et al.* (9). Surprisingly, this composite pulse has been little used in materials science investigations. The very large RF power required for large samples, and the consequent power dissipation and tissue heating *in vivo*, have discouraged its use in biomedical applications. The method consists of a  $\pi/2$  nonselective pulse sandwiched between the leading and

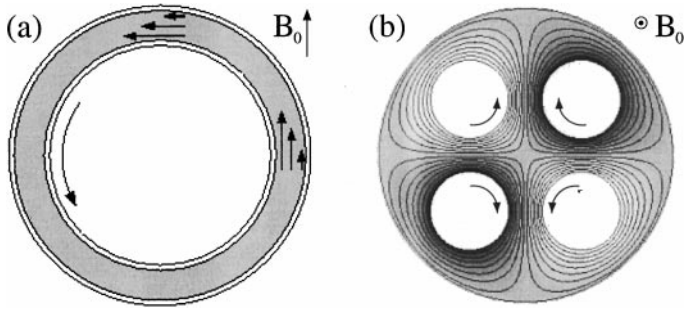


**FIG. 1.** Cross-sectional views of rheometric devices: (a) horizontal Couette cell; (b) four-roll mill extensional flow apparatus. Arrows indicate the direction of mechanical driving, with fluid streamlines shown for the four-roll mill.

trailing halves of a  $\pi/2$  sinc pulse of opposite phase. We refer to this pulse sequence here as “split-sinc selective storage,” or S4. Spins having local frequencies which fall within the bandwidth of the selective pulse experience a zero net tip angle, while spins outside the desired region are affected only by the nonselective pulse and are immediately subjected to a large dephasing gradient. As we are not performing multislice experiments, our only interest in the extraslice spins is in ensuring they do not contribute to the signal. Following the dephasing gradient the only coherent magnetization remaining lies within the pulse profile and is preserved along the  $z$  axis for later recall. The stored  $z$ -magnetization is subject only to the much less severe effects of longitudinal relaxation.

A comparative study of profiles resulting from several volume-selective pulse techniques (10) indicates that well-defined profiles may be achieved using the pulse cluster described above. While we investigated the relevant magnetization trajectories for several selection techniques and found the split-sinc selective storage pulse scheme particularly suitable in the case of spin systems for which  $T_2 \ll T_1$ , we do not attempt a comprehensive comparative study here. We do compare its associated magnetization trajectories and resulting profiles to those for an alternate method of  $z$ -storage consisting of a standard refocused  $\pi/2$  sinc selective pulse followed by a  $-\pi/2$  nonselective storage pulse. We do this simply to point out the significant advantage, in severe  $T_2$  situations, of S4 over selective techniques employing sinc excitation pulses. We then focus on our application of this approach in the Rheo-NMR geometries shown in Fig. 1.

The magnetization trajectories are investigated by solving the Bloch equations in the rotating frame of the RF pulse, in which the local  $z$ -component of magnetic field experienced by a nuclear spin is offset by  $G_x x$ , where  $G_x$  is the field gradient strength at position  $x$  from the slice center. A fourth-order Runge–Kutta algorithm (11) was employed here to find numerical solutions and thereby simulate the response of the spin system to an arbitrary RF excitation. As we found it instructive to follow the magnetization trajectory during and following the selective pulses, we obtained the complete time evolution of  $M_x$ ,  $M_y$ , and  $M_z$  everywhere within and outside the slice profile. The calculations

presented here are for 2-ms three-lobe sinc selective pulses, starting magnetization vector  $M = [0, 0, 1]$ , and values for gradient strength and hard pulse duration appropriate for our hardware (12).

The time evolution of in-slice magnetization, during the preparation along  $z$  and the subsequent large dephasing gradient, is shown in Fig. 2. For the S4 pulse cluster,  $M_z$  is only momentarily tipped toward the transverse plane (Fig. 2a) and is successfully prepared along  $z$  before the large spoiler gradient is applied. Consequently, the signal in the spatial profile is almost entirely preserved even when  $T_2$  conditions are severe. This is impressive when compared to sinc pulses (Fig. 2b) for which the magnetization undergoes a large excursion into the transverse plane where it remains for almost the entire second

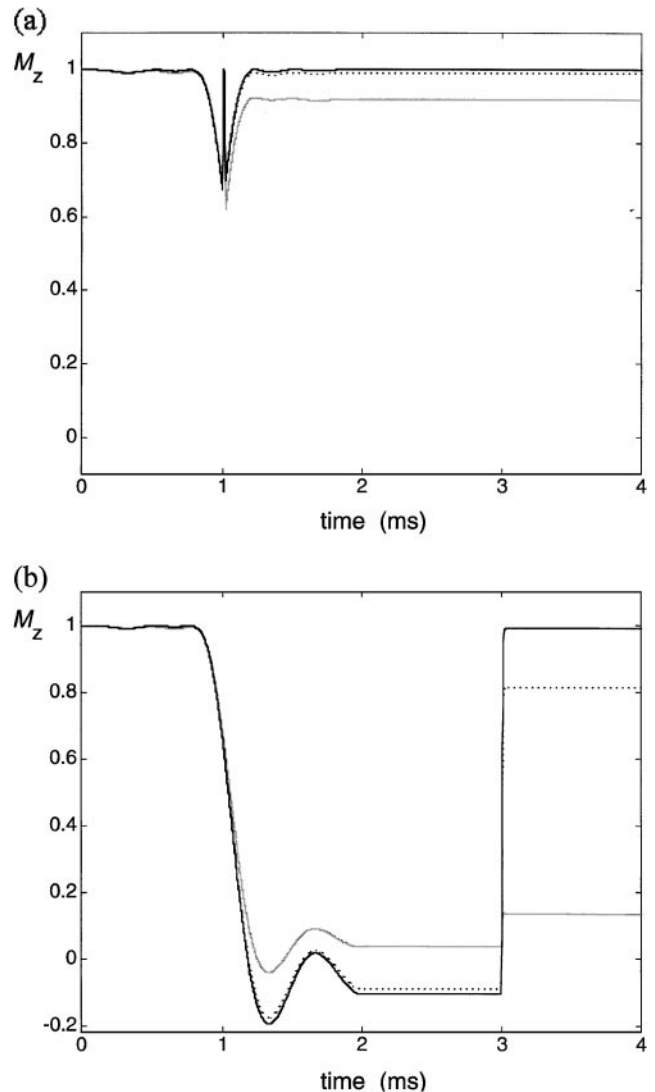


**FIG. 2.** Simulated time evolution of in-slice magnetization  $M_z$  for (a) S4 and (b)  $(\pi/2)_{\text{selective}}[-\pi/2]z$ -storage for  $T_2 = 1$  s (black solid lines),  $T_2 = 10$  ms (dotted lines), and  $T_2 = 1$  ms (gray lines). The selective pulses are 2-ms three-lobe sinc pulses.

half of the pulse. When  $T_2$  is on the order of 1 ms, less than 20% of the in-slice magnetization is recoverable following the  $z$ -storage. For selection techniques employing sinc excitation pulses, the resulting loss of signal in the magnetization profile can be dramatic, especially when the nature of the experiment requires selection in more than one direction. Figure 3 compares the calculated profiles following two successive applications of the selection, for a typical total  $z$ -storage duration of 8 ms. For the calculations using  $T_2 = 10$  ms shown in Fig. 3a, both profiles are well-defined. However, the S4 pulse sequence preserves 98% of the in-slice magnetization, compared to 67% for the refocused sinc pulse. The comparison is much more dramatic for the extreme case of  $T_2 = 1$  ms (Fig. 3b). The split-sinc pulse profile is now less sharply defined, yet a full 84% of the starting

signal is preserved in the profile. In contrast, the sinc profile has been reduced to 2% of its original signal.

Based on the excellent performance of S4 in terms of rectangular slice profile and short exposure of  $M_z$  to transverse dephasing, we incorporated it into a method of doing spatially selective spectroscopy. Using this selective storage precursor along with the appropriate NMR spectroscopy experiment, we obtain direct spatial information about flow-induced alignment.

## MATERIALS

We discuss here results from a polymer melt, 610-kDa poly(dimethylsiloxane), under steady shear. The NMR interaction parameters are the proton dipolar and deuterium quadrupolar interactions. These are both orientation-dependent and so are sensitive to anisotropy in the average orientation of the polymer segments. In the case of the deuterium quadrupolar experiments the alignment of the main-chain polymer is directly reported on by a deuterated oligomer probe molecule via a *pseudo-nematic* interaction (13). Because it experiences the same orientational field as the main chain, the probe reports directly on the polymer segmental alignment.

The shear experiments were carried out in a Couette cell having 5-mm inner cylinder diameter, a gap of 0.5 mm containing the sample, and an RF coil mounted directly on the outer cylinder. This entire apparatus was mounted on a NMR microimaging probe (Bruker) and inserted in a 7-T vertical bore magnet. The mechanical driving of the shear was performed via a drive shaft from the top of the magnet. The velocity in the tangential direction of the Couette cell, and the velocity gradient in the radial direction, define axes of the hydrodynamic frame. The third axis is colinear with the long axis of the Couette and is perpendicular to the magnetic field direction in these experiments. Under shear, polymer segments experiencing anisotropy will align at some angle to these axes. The horizontal Couette provides an opportunity to distinguish between, and obtain alignment information from, different orientations of the hydrodynamic frame with respect to the lab frame.

## SPECTROSCOPY

In solids and liquid crystals the quadrupolar interaction strengths are hundreds of Kilohertz, and the splittings are easily resolved. In contrast, flow-induced alignment of polymer segments is extremely weak, and furthermore the probe molecule reports a scaled order parameter. The resulting quadrupolar splittings are on the order of tens of hertz and observing them becomes a delicate matter since the intrinsic linewidth is approximately 100 Hz in the acquisition domain. Hence, in the Couette experiments, rather than perform a straightforward solid echo we acquired two-dimensional spectra as described in Fig. 4. A series of Hahn echoes was collected wherein the delay time  $t_1$  was incremented to define the evolution domain. The Hahn echo refocuses all Zeeman effects, and the second rank tensorial

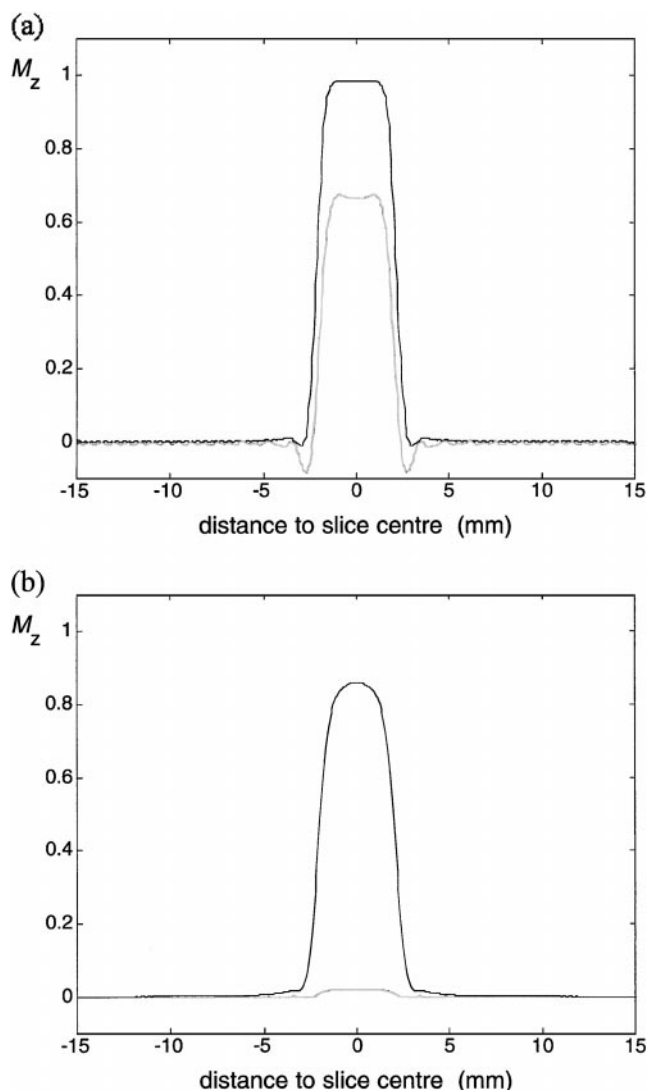


**FIG. 3.** Profiles across the desired slice following two successive applications of the S4 (shown in black) and refocused sinc (gray)  $z$ -storage methods, representing selection in two orthogonal directions in strongly relaxing spin systems: (a)  $T_2 = 10$  ms; (b)  $T_2 = 1$  ms.

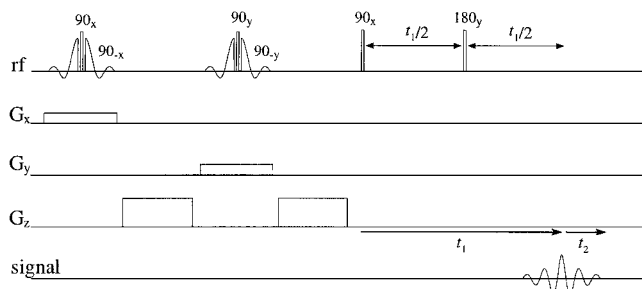


**FIG. 4.** Pulse sequence showing two applications of the selective storage cluster followed by the two-dimensional spectroscopy experiment. The spoiler gradient shown here is applied along  $z$ ; however, it may equally be applied in any (or all) of the three orthogonal directions following the  $z$ -storage.

interactions remain to modulate the echo. With careful choice of  $t_1$  and properly phased spectra, the amplitude of the echo peak undergoes a cosine modulation along the evolution domain. The frequency of the modulation corresponds to the strength of the remaining (here, quadrupolar) interaction, which appears as a splitting in the evolution domain Fourier transform. Figure 5 shows representative spectra obtained in the horizontal Couette. Images taken with the selective storage precursor to confirm its selectivity are also shown. We determined that the polymer melt under shear may undergo a “supramolecular” ordering along the velocity gradient direction. These results have been published in (14).

### REMARKS ON IMPLEMENTATION

There were several difficulties encountered when we implemented the S4 technique. Of particular note are the switching times for the pulse phase and those for the gradients. The

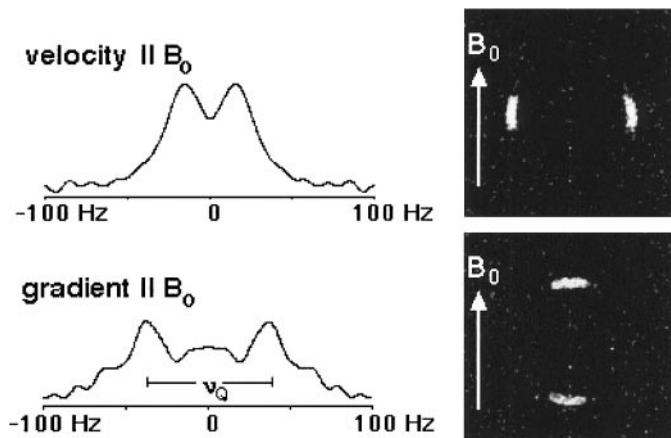


**FIG. 5.** Molecular alignment within the shear plane was explored by limiting the Hahn echo experiments to small arcs of the flow field in the Couette depicted in Fig. 1a. The top spectrum was obtained from the sides of the 0.5-mm Couette gap, where the velocity direction is parallel to the magnetic field (observation) direction. The lower spectrum corresponds to the top and bottom of the Couette where the velocity gradient direction is parallel to  $B_0$ .

frequency-selective and broadband RF pulses are transmitted via low- and high-power amplifiers, respectively. These pulses must also be of opposite phase. While switching between the amplifiers is very fast on the AMX-300 spectrometer, the phase of the pulse could not be switched within an acceptable length of time. To avoid this, the leading and trailing halves of the selective pulse are provided to the spectrometer as negative waveforms. The effect of switching the phase is thus achieved without experiencing the associated hardware delays.

The profiles in Fig. 3 show the ideal situation in which the magnetic field gradient can be removed during the application of the hard pulse. This also presents a hardware challenge, as

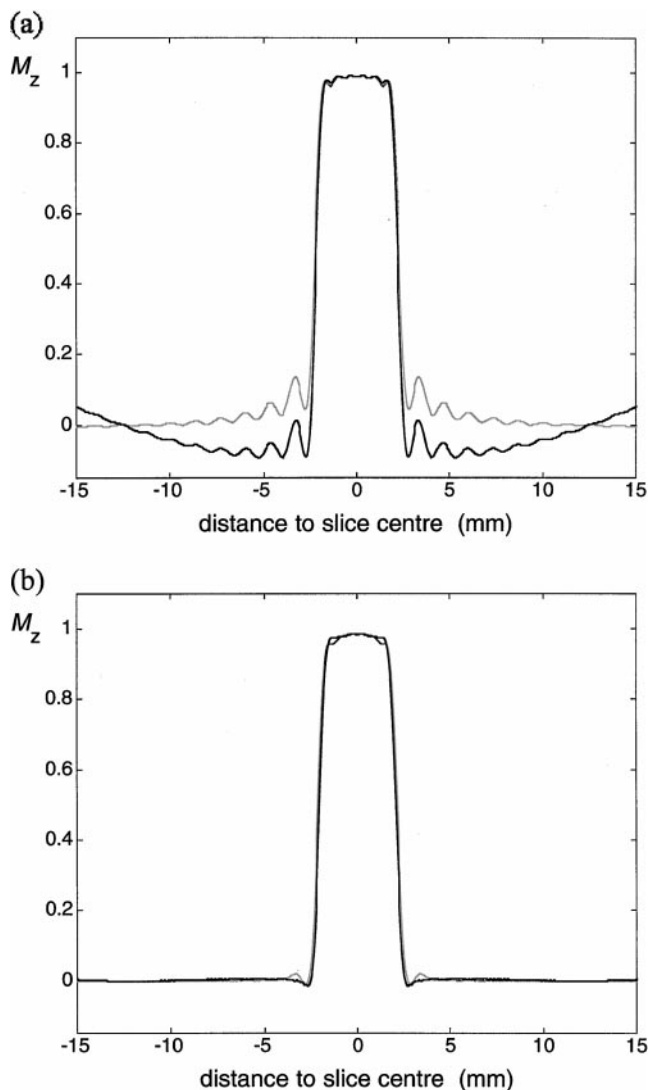


**FIG. 6.** Numerical results for distorted slice profile (shown in black) corresponding to application of the nonselective pulse in the presence of the magnetic field gradient. The profile is compared to that obtained with magnetic field gradient removed during the application of the broadband pulse (gray). The simulated profiles obtained for two applications of S4 are shown in (b).  $T_2 = 10$  ms in these calculations.

the time needed for the gradients to be reliably turned on or off is hundreds of microseconds. Alternatively, the gradient is not allowed to fall until the desired magnetization has been prepared along  $z$ . The delivery of the broadband pulse in the presence of the gradient imparts a sinc modulation to the desired profile. The slice remains sharply bounded but the baseline suffers a distortion, as shown in Fig. 6a. This corresponds closely to what we observe in experimental profiles. According to our numerical results in Fig. 6b, a second application of the selection along the same direction should eliminate the distortion. In practice, it is not always possible to completely eliminate extraslice signal in this way. The severity of the sinc distur-

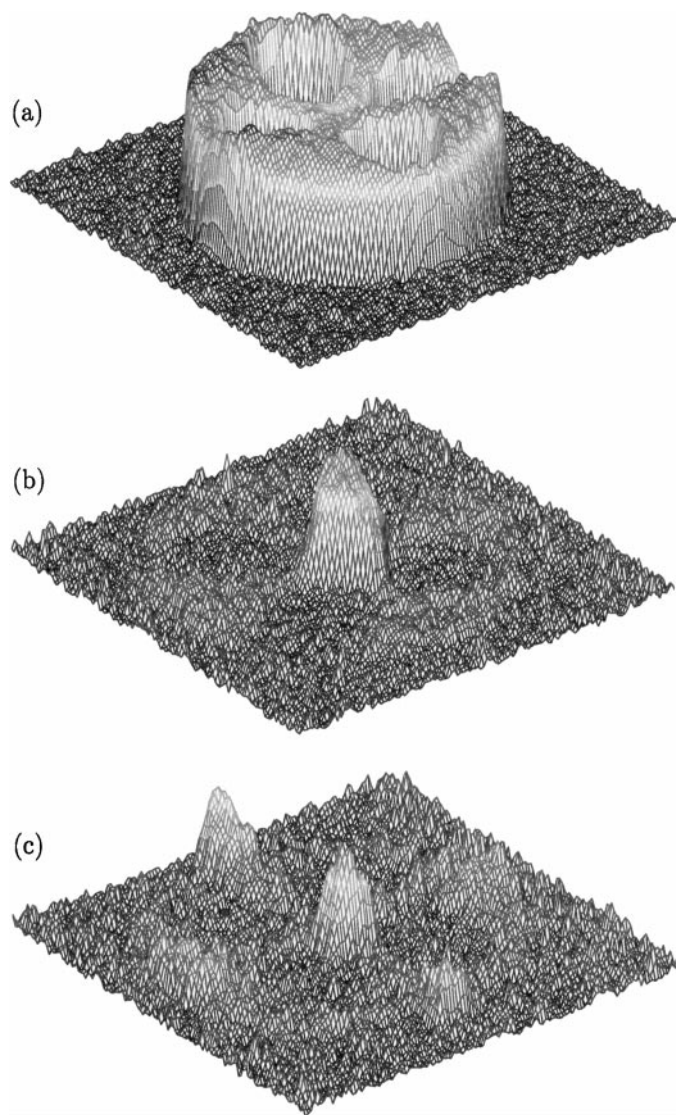


**FIG. 7.** Experimentally determined spatial profiles of polymer liquid crystal in deuterated solvent, in the four-roll mill: (a) a 2-mm layer of fluid; (b) selection in two orthogonal directions to obtain signal from a  $(4 \text{ mm})^2$  region in the center of the 18-mm-diameter cell; (c) selection of  $(2.5 \text{ mm})^2$  region results in significant signal from the extraslice wings. The images were obtained using a 20-mm  $^2\text{H}$  saddle coil.

tion scales with the gradient strength and with the duration of the broadband pulse, which in turn depends on the quality factor of the resonator or coil used to deliver the RF power. For a given desired slice width and broadband pulse duration, a shorter selective pulse requires a larger field gradient, leading to narrowing of the undesirable “wings” toward the desired slice. This trade-off, and not the upper limit of the gradient strength itself, determines the selective resolution obtainable on our spectrometer.

The limitations imposed by these conditions are highlighted in Fig. 7. In this case the selective storage method is used to obtain critical alignment information for a polymer liquid crystal, poly( $\gamma$ -benzyl-L-glutamate) in dioxane/nitrobenzene, in the four-roll mill apparatus. The region of interest is in the center of this device where the flow closely approximates a stagnation flow and can produce large extension of the polymer chains. We are able to achieve signal exclusively from a very well-defined region of  $(4 \times 4 \text{ mm})$  (Fig. 7b). At still larger gradient strength for a selected region of side length 2.4 mm, the desired region remains well defined but the contribution to the spectrum from the wings (Fig. 7c) will be unacceptable.

In each of a series of acquisitions, we normally use large dephasing gradients and more than one application of the storage precursor, either to select in two or three dimensions or to minimize the unwanted signal from the sinc wings. Used in this way the method is very demanding of the field gradient coils. Care must be taken to monitor their temperature and to allow sufficient time between acquisitions. If possible, air cooling should be used to prevent damage to the gradients and also to avoid temperature variations in the sample during the experiment.

## CONCLUSION

We have shown that the S4 selective storage method is well-suited to spatially localized spectroscopy in strongly relaxing spin systems. Its utility is limited, however, by the particular hardware available and we have indicated means by which switching delay times can be avoided by using a constant gradient and constant phase setting during the RF excitation process. Compensation techniques to improve the slice profile, as suggested by Müller *et al.* (15), have not been attempted in these experiments and might be incorporated in future. While we have tailored this method to suit our Rheo-NMR methods, it can easily be extended to a wide range of applications. For example, we have also used the S4 precursor in velocity imaging and we have found it particularly valuable as a slice selection tool in echo planer imaging experiments. Its distinguishing features are that it may be added as a slice selection precursor to any pulse sequence consisting entirely of hard pulses, that its effect may be easily ascertained by subsequent imaging, and that it is found to be extraordinarily robust against  $T_2$  relaxation.

## ACKNOWLEDGMENTS

The authors are grateful to the New Zealand Foundation for Research, Science, and Technology, the Royal Society of New Zealand, the Marsden Fund, and the Natural Sciences and Engineering Research Council of Canada for financial support and to Michael Morrow for informative discussions.

## REFERENCES

1. P. A. Bottomley, U.S. Patent 4,480,228, October 1984; P. A. Bottomley, T. B. Foster, and R. D. Darrow, *J. Magn. Reson.* **59**, 338 (1984).
2. J. Frahm *et al.*, German Patent DE-3445689, 1984; J. Frahm, K. D. Merboldt, W. Hänicke, and A. Haase, *J. Magn. Reson.* **64**, 81 (1985).
3. D. M. Doddrell, W. M. Brooks, J. M. Bulsing, J. Field, M. G. Irving, and H. Baddeley, *J. Magn. Reson.* **68**, 367 (1986); D. M. Doddrell, J. M. Bulsing, G. J. Galloway, W. M. Brooks, J. Field, M. G. Irving, and H. Baddeley, *J. Magn. Reson.* **70**, 319 (1986).
4. R. Kimmich and D. Hoepfel, *J. Magn. Reson.* **72**, 379 (1987).
5. H. Geen, S. Wimperis, and R. Freeman, *J. Magn. Reson.* **85**, 620 (1989).
6. P. T. Callaghan and E. T. Samulski, *Macromolecules* **30**, 113 (1997).
7. D. A. Grabowski and C. Schmidt, *Macromolecules* **27**, 2632 (1994).
8. H. Post, D. Ratzel, and P. Brunner, West German Patent P3209263.6, 13 March 1982.
9. W. P. Aue, S. Müller, T. A. Cross, and J. Seelig, *J. Magn. Reson.* **56**, 350 (1984); S. Müller, W. P. Aue, and J. Seelig, *J. Magn. Reson.* **63**, 530 (1985).
10. J. Frahm and W. Hänicke, *J. Magn. Reson.* **60**, 320 (1984).
11. W. H. Press, B. P. Flannery, S. A. Teukolsky, and W. T. Vetterling. "Numerical Recipes: The Art of Scientific Computing," Cambridge Univ. Press, Cambridge, 1986.
12. For slice selection a gradient strength of 0.0176 T/m was used in the numerical solutions, corresponding to 5% of the maximum gradient strength available for our gradient supplies. 25% gradient strength or 0.088 T/m was used for the 1-ms spoiler gradients. In the calculations we also used  $B_1$  field strength corresponding to a 20- $\mu$ s nonselective  $\pi/2$  pulse.
13. H. Toriumi, B. Deloche, J. Herz, and E. T. Samulski, *Macromolecules* **18**, 304 (1985).
14. P. T. Callaghan, M. L. Kilfoil, and E. T. Samulski, *Phys. Rev. Lett.* **81**, 4524 (1998).
15. S. Müller, W. P. Aue, and J. Seelig, *J. Magn. Reson.* **65**, 332 (1985).